European Journal of Pharmaceutics and Biopharmaceutics 71 (2009) 207–213

Contents lists available at ScienceDirect

European Journal of Pharmaceutics and Biopharmaceutics

journal homepage: www.elsevier.com/locate/ejpb

Research paper

Benefits of nanoencapsulation for the hypercin-mediated photodetection of ovarian micrometastases

Magali Zeisser-Labouèbe, Florence Delie, Robert Gurny, Norbert Lange *

Department of Pharmaceutics and Biopharmaceutics, School of Pharmaceutical Sciences, University of Geneva, University of Lausanne, Geneva, Switzerland

ARTICLE INFO

Article history:
Received 11 July 2008
Accepted in revised form 2 October 2008
Available online 17 October 2008

Keywords:
Ovarian cancer
Fluorescence photodetection
Nanoparticle
Hypericin
In vivo
Drug delivery system

ABSTRACT

The high recurrence and lethality of ovarian cancer at advanced stages is problematic, especially due to the development of numerous micrometastases scattered throughout the abdominal cavity. Fluorescence photodetection (PD) used in combination with surgical resection of malignant tissues has been suggested to improve recovery. Based on promising *in vivo* results for the detection of bladder cancer, hypericin (Hy), a natural photosensitizer (PS), stands as a good candidate for the photodetection of ovarian cancer. However, due to its hydrophobicity, systemic administration of Hy is problematic. Polymeric nanoparticles (NPs) help to overcome these delivery and stability problems and enable intravenous administration of Hy. In this study, Hy-loaded NPs of polylactic acid were produced with the following properties: (i) mean size of 268 nm, (ii) negative zeta potential, (iii) low residual surfactant and (iv) drug loading of 3.7 % (w/w). The potential of hypericin-loaded nanoparticles for the fluorescence photodetection of ovarian metastases in Fischer 344 rats bearing ovarian tumours was compared to free drug. The selectivity of Hy administered with both formulations was assessed first by fluorescence endoscopy, and then quantified after tissue extraction. The results showed an improved selective accumulation of Hy in ovarian micrometastases when NPs were used.

1. Introduction

One out of six cancer cases among women in the world is of gynaecological origin [1]. Ovarian cancer ranks fifth amongst the most fatal forms of female cancer in Europe and the United States [2,3]. It causes more deaths than any other cancer of the female reproductive system in the developed countries [1]. In the US, 22 430 new cases and 15 280 deaths were projected to occur in 2007 [3]. The high proportion of deaths reflects the poor prognosis for this disease. Indeed, the mean five-year survival rate is 45%, but mainly depends on the stage at diagnosis [3]. The 5-year relative survival rate is 93% if diagnosed early and decreases to 30% for advanced stages. Unfortunately, only 19% of all cases are detected at the early stages due to the absence of early warning signs or obvious symptoms. Even if the epidemiology of ovarian cancer is better understood, today, no significant progress with respect to mortality has been made in contrast to other cancers such as breast cancer [3]. Routine screening is not yet available for the early detection of ovarian cancer and tests such as tumour marker CA125 level, transvaginal ultrasonography and pelvic examination, alone or in combination, are not specific and sensitive enough for women of normal risks [4,5]. In most cases, an initial laparotomy is performed for histological analysis of all suspicious sites for reliable diagnosis. Depending on the stage of the diagnosed disease, various combination schemes of taxane- and platinum-based chemotherapy are used with the aim of complete clinical remission. Still, high recurrence rates are one of the key issues for women diagnosed with advanced ovarian cancer. The relapse and associated lethality of ovarian cancer are mainly due to the dissemination of ovarian micrometastases in the entire peritoneal cavity at the advanced stages of the disease [6]. In these cases, surgery and subsequent chemotherapy are generally not effective enough to suppress all the ovarian cancer metastases. One of the explored strategies to increase the efficacy of the treatment is to enhance the detection of malignant cells during surgery. Fluorescence photodetection (PD) using photosensitizers (PS) appeared as a potent technique to optimise lesion resection with a minimal damaging rate of normal tissue [7] and has been recently shown to significantly reduce recurrence in bladder cancer patients [8]. After PS administration, subsequent accumulation in the malignant tissue and activation by light, clinicians could ideally remove the abnormal tissues which would be highlighted by their red fluorescence. In the early 1950s, the use of porphyrins, such as haematoporphyrin and its derivatives, was first reported for preferential tumour localisation [9]. Currently, PS such as Photofrin®, 5-aminolevulinic acid (5-ALA)-mediated protoporphyrin IX and Foscan® are

* Corresponding author. Department of Pharmaceutics and Biopharmaceutics, School of Pharmaceutical Sciences, University of Geneva, University of Lausanne, 30, Quai E. Ansermet, CH-1211 Geneva 4, Switzerland. Tel.: +4122 379 3335; fax: +4122 379 6567.
E-mail address: Norbert.Lange@pharm.unige.ch (N. Lange).

0939-6411/$ - see front matter © 2008 Elsevier B.V. All rights reserved.
doi:10.1016/j.ejpb.2008.10.005

commercially available and used for gynaecological applications. Regarding ovarian cancer, fluorescence photodetection has been studied with 5-ALA and its derivatives *in vivo* on rats [10–15] and humans [16–18]. However, most PS still suffer from several drawbacks such as low selectivity, high drug dose, skin photosensitisation and unsuitable PS administration and delivery systems [19–21]. Progress in the field of photodetection of ovarian cancer is still needed and optimisation of PS delivery represents one alternative.

Hypericin (Hy) is a natural compound belonging to the class of phenanthroperylenequinones, and is extracted from the plant *Hypericum perforatum*, found worldwide [22,23]. The photoactivity of Hy has been demonstrated *in vitro* and *in vivo* on different experimental animal models [24–31]. Hy is not only a potent photosensitizer for photodynamic therapy (PDT), but also a fluorescent drug for PD with a high fluorescence quantum yield [32]. One other advantage of Hy over other PS is its low photobleaching [33,34], as shown during extensive investigations on the fluorescence detection of bladder cancer [33–35]. The potential of Hy was shown in the chick chorioallantoic membrane model with favorable bladder tumour-to-normal tissue ratios [36] and in humans providing a high sensitivity and specificity for detecting bladder cancer cells [37–39]. Based on these promising results, Hy stands as a good candidate for the photodetection of ovarian cancer. Since the peritoneal cavity is not easily accessible in a pre-surgery setting, Hy should ideally be administered systemically. However, Hy lipophilicity makes formulation difficult due to the lack of physiologically acceptable solvents [20,40]. Therefore, the design of adequate delivery systems for Hy is critical for improving the outcome and acceptability of PD in a clinical context. Different formulations of Hy have been investigated using nontoxic pharmaceutical additives such as *N*-methyl pyrrolidone, polyvinylpyrrolidone, polyethyleneglycol, proteins or colloidal carriers such as emulsions or liposomes [38,41–46]. Furthermore, polymeric nanoparticles have been suggested to improve the delivery of Hy [20,47]. In a previous study, we have demonstrated the efficacy of this delivery system *in vitro* with ovarian cancer cells [48].

In the present study, we first produced and characterised Hy-loaded PLA NPs in terms of size and drug loading. Following, the feasibility of fluorescence photodetection using the Hy encapsulated in NPs was evaluated in comparison to free Hy on ovarian cancer-bearing Fischer 344 rats [10,49]. The selective accumulation of Hy was qualitatively determined by fluorescence endoscopy, and then quantified by tissue extraction.

2. Materials and methods

2.1. Animals

Female Fischer rats F-344 (150–200 g) were obtained from Charles River Laboratories (L'Arbresle, FR), and housed in a pathogen-free animal facility. They were given commercial basal diet and water *ad libitum*. All the aspects of the animal experiment and husbandry were carried out in compliance with the national regulations and approved by the cantonal veterinary office of Geneva, Switzerland.

2.2. Cell line and tumour implantation

The NuTu-19 cell line, a poorly differentiated Fischer 344 rat-derivative epithelial ovarian cancer cell line was kindly provided by Dr. A. Major [10,49]. Cells were maintained in DMEM medium (Gibco Life Technologies, Carlsbad, US) supplemented with 10% fetal calf serum (FCS, Brunschwig, Amsterdam, NL) and 100 U/ml penicillin–streptomycin (Gibco Life Technologies, Carlsbad, US) at 37 °C in a 5% CO_2 atmosphere. Before tumour implantation, NuTu-19 cells were washed twice with PBS (Gibco Life Technologies, Carlsbad, US), harvested using 0.5 % Trypsin-EDTA (Gibco Life Technologies, Carlsbad, US) and counted. After centrifugation, a suspension in an equal mixture of complete culture medium and Matrigel™ matrix (BD Biosciences, Bedford, US) was prepared. One million cells in 1.5 ml were intraperitoneally injected into the Fischer rats ($n = 20$), and tumour development was allowed for 5 weeks.

2.3. Photosensitizer formulation and characterisation

Hypericin (Hy, purity ⩾ 98%) was provided by Alexis Corporation (Lausen, CH). A stock solution of Hy was prepared in ethanol (Fluka Chemie AG, Buchs, CH) at 5 mg/ml and stored at −20 °C in the dark. Two formulations of Hy were compared for *in vivo* studies. Hy was either dissolved in a mixture of ethanol, polyethyleneglycol 400 (PEG, Merck, Hohenbrunn, DE) and water (2:3:5) or incorporated into polymeric nanoparticles. Polylactic acid (PLA) was obtained from Lakeshore Biomaterials, Inc. (Birmingham, US). Poly(vinyl alcohol) (PVAL) (Mowiol 4–88) from Hoechst (Frankfurt/M, D) was used as a surfactant.

The nanoparticles of PLA were produced by the nanoprecipitation method as previously described [48]. Briefly, an organic phase containing PLA (100DL 4A, 54 kDa) and Hy dissolved in acetone was poured under magnetic stirring into an aqueous PVAL solution (0.4%, w/w). The organic solvent was evaporated under atmospheric pressure at room temperature, and the NPs were purified by centrifugation (Beckman, Avanti™ 30, Fullerton, US). Finally, NPs were freeze-dried (Edwards, Modulyo, Oberwil, CH) with D(+)-trehalose dihydrate (Sigma Chemical, St. Louis, US) as a lyoprotectant and stored at +4 °C until use.

NPs were characterised in terms of size and drug loading. The mean size was determined by photon correlation spectroscopy using a Zetasizer® 3000HS (Malvern instruments, Worcestershire, UK). The zeta potential was measured in 10^{-3} M NaCl using the electrophoretic mode with the Zetasizer® 3000HS. The drug loading was determined by reversed-phase HPLC after solubilization of NPs in acetone (Fluka Chemie AG, Buchs, CH) as previously described [48]. The residual PVAL was determined using a method based on the formation of a stable complex of PVAL with iodine in the presence of boric acid [50].

2.4. Fluorescence imaging

Before administration to tumour-bearing rats, dilutions of free Hy in a mixture of ethanol, PEG 400 and water for free Hy or Hy encapsulated in NPs in NaCl 0.9% (Bioren SA, Couvet, CH) were freshly prepared. Hy was administered intravenously in the tail vein to the tumour-bearing rats at a dose of 2 mg/kg.

To determine the accumulation of Hy in tumour tissues, the rats were sacrificed by CO_2 asphyxia 3, 6 and 24 h after Hy administration ($n = 3$). The abdominal cavity was opened to reach the tumour for fluorescence imaging using a D-light system® (Karl Storz GmbH & Co. KG, Tuttlingen, DE) connected to a CCD camera (Telecam SL-PDD, Karl storz GmbH & Co. KG, Tuttlingen, DE). Images were compared under white and blue light.

2.5. Determination of hypericin concentration in tissues and blood

Blood and tissue samples (tumour, surrounding muscles, liver, spleen and lung) were collected from Fischer rats, 3, 6 and 24 h after Hy administration, weighted and kept at −20 °C until analysis. Control samples were also taken from rats receiving no drug. The tissues were homogenised with tetrahydrofuran (THF) with a tissue homogeniser (Eurostar digital, IKA®-Werke, Staufen, DE).

The blood samples were extracted with THF under sonication five times for 5 s (sonifier S-450D®, Branson Ultrasonic S.A, Geneva, CH). After centrifugation, the supernatants were evaporated under nitrogen. The residues were dissolved in 0.3 ml DMSO. The fluorescence was determined with a microplate reader (Safire®, Tecan, Salzburg, AT) with excitation and emission wavelengths set at 530 and 645 nm, respectively. The background fluorescence of control samples, taken on rats receiving NaCl 0.9%, was subtracted. The Hy concentration was calculated from the calibration curve (0.04–10 μg/ml).

2.6. Statistical analysis

Values of Hy concentrations and ratio of Hy concentrations between tumour and surrounding muscles are expressed as the mean ± SD, and the significance of the differences was calculated by Student's t test. Values of $p < 0.05$ were considered as significant.

3. Results

3.1. Nanoparticle characterization

NPs with a mean diameter of 268 nm (polydispersity index of 0.121) and a negative zeta-potential (-28 mV) were obtained by nanoprecipitation. A high entrapment efficiency of Hy (74%) was achieved to reach a drug loading of 3.7%. As PVAL, used as a surfactant, is reported to be non-biodegradable, its intravenous administration should be minimised as much as possible. For this purpose, a step of purification by centrifugation was added. The residual PVAL was as low as 6% (w/w) on the freeze-dried NPs. This minimal residual amount of PVAL, as a thin hydrophilic layer around NP, is necessary to allow the redispersion of NPs in aqueous solution after freeze-drying.

3.2. Fluorescence imaging

The abdominal cavity of Fischer rats was opened at 3, 6 and 24 h after Hy administration (2 mg/kg), either in solution (free Hy) or as NP suspension, and the distribution of Hy was visualised by endoscopy under white and blue light (Fig. 1). The intraperitoneal injection of NuTu-19 cells in a mixture of cell culture medium and matrigel™ resulted in the tumour development in 100 % of rats (see Supplementary information). Indeed, tumour nodules of a few mm were scattered in the entire peritoneal cavity either individually or forming omental tumour masses. Tumour nodules were found adherent to the different parts of the abdomen such as abdominal wall, diaphragm, bowel, liver and spleen. Furthermore, the presence of a haemorrhagic malignant ascite of dozens of ml was observed 5 weeks after tumour implantation. 3 h after admin-

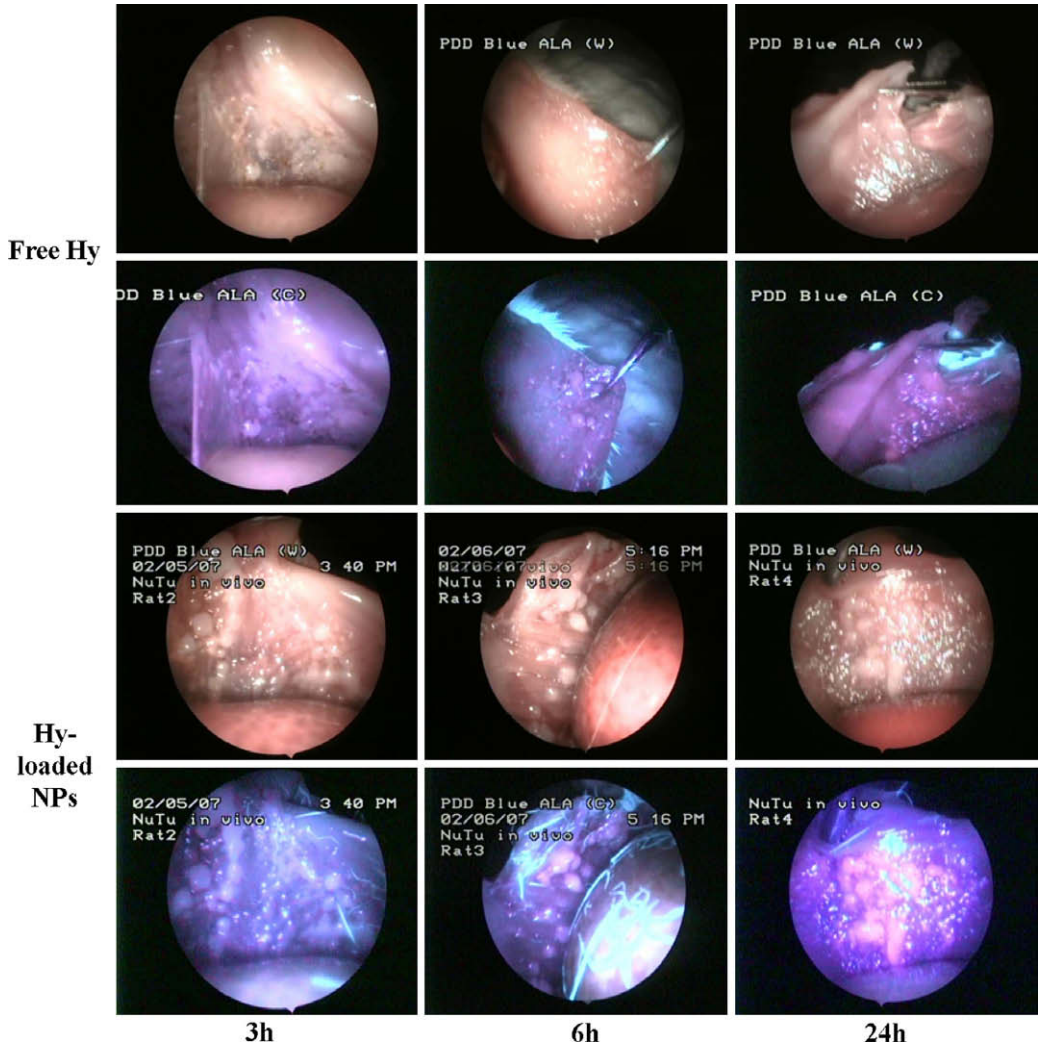

Fig. 1. Images of ovarian metastases at different times after iv administration of free Hy or Hy-loaded NPs under white light and under blue light.

istration, under blue light, a slight red fluorescence from tumour nodules was already visible with both formulations (Fig. 1). At 6 or 24 h, no visible contrast between tumours and surrounding muscles could be observed with free Hy. On the contrary, with NPs, the fluorescence contrast increased as a function of time post-administration. Twenty-four hours after Hy-loaded NP administration, tumour nodules exhibited a bright red fluorescence. The contrast of fluorescence and thus the selectivity for tumours were higher when NPs were used as compared to the solution. With both formulations, no photobleaching was observed during the investigation time (15–30 min).

3.3. Hy biodistribution

To further quantify the drug distribution as a function of the formulation, Hy was extracted from different tissues collected at 3, 6 and 24 h after iv injection (2 mg/kg). The blood clearance was faster for free drug (Fig. 2A). Hy encapsulated in NPs had a longer circulation time with a peak at 6 h. A substantial amount of Hy-loaded NPs were taken up by the liver and spleen (Fig. 2B/C).

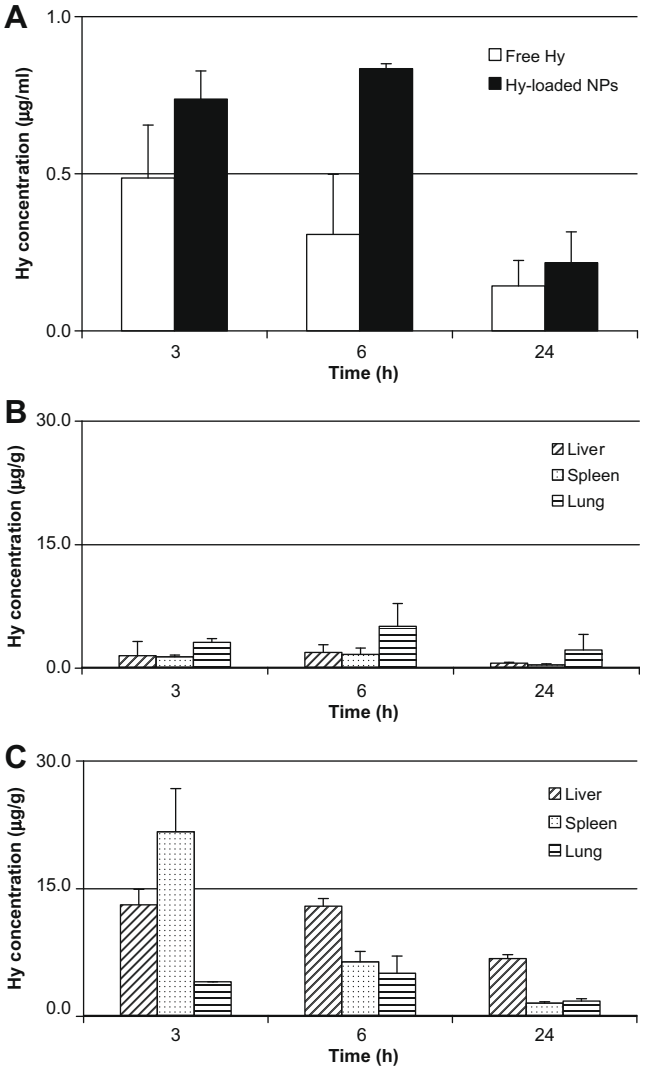

Fig. 2. Biodistribution profile of Hy after iv administration at a dose of 2 mg/kg to Fischer F-344 rats bearing NuTu-19 tumours. (A) Plasma concentration profile, expressed as µg Hy per ml of blood, of free Hy or Hy-loaded NPs. Hy concentration as a function of time in different organs, expressed as µg Hy per g of tissue, after administration of free Hy (B) or Hy-loaded NPs (C). Each data point represents the mean (±SD) of three animals.

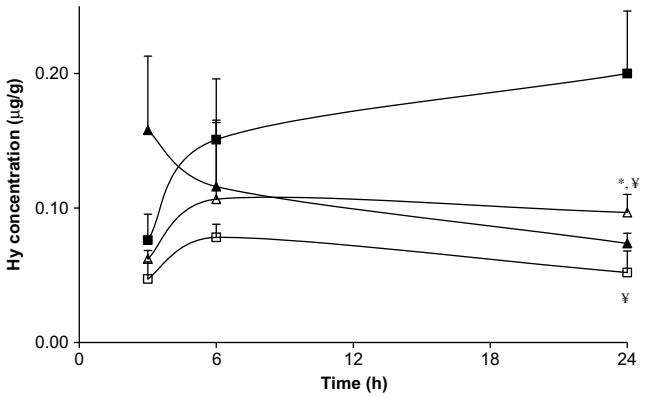

Fig. 3. Tissue distribution of hypericin, expressed as µg Hy per g of tissue, in the tumour (dark symbols) and in the surrounding muscle (open symbols) at different times after iv administration of free Hy (▲) or Hy-loaded NPs (■) at a dose of 2 mg/kg to Fischer F-344 rats bearing NuTu-19 tumours. Each data point represents the mean (±SD) of three animals. *Significantly different from Hy concentration in the surrounding muscle (Student's t test, $p < 0.05$). ¥Significantly different from rats injected with free Hy (Student's t test, $p < 0.05$).

However, Hy was effectively removed from these tissues as the concentration rapidly decreased. Similar levels were measured in the lung for free Hy and Hy-loaded NPs.

Tumour selective localisation, as observed with endoscopy, was confirmed by analysis of Hy concentration in tumours and surrounding muscles over the time, as shown in Fig. 3. For the free drug, tumour concentration was maximal after 3 h and decreased thereafter leading at 6 h to a lower Hy concentration in tumour than in muscle. With NPs, tumour concentration gradually increased, and the highest value was observed at 24 h. After 3 h, the muscle concentration was significantly higher after free Hy administration than following administration of Hy-loaded NPs. Moreover, the muscle concentration decreased faster when NPs were used, confirming the rapid elimination from healthy tissues. To corroborate the selectivity of Hy for malignant tissues, tumour to muscle ratios were calculated for both formulations (Fig. 4). More selective accumulation in ovarian micrometastases was achieved with NPs as compared to free drug. Indeed, the maximal tumour-to-muscle ratios were observed for free Hy at 3 h postinjection (t/m ratio = 2.3) and for Hy-loaded NPs at 24 h (t/m ratio = 3.5).

4. Discussion

The high recurrence and lethality of ovarian cancer at advanced stages is problematic, especially due to the development of numer-

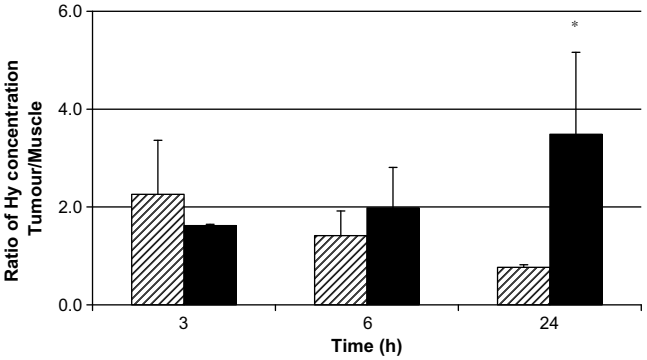

Fig. 4. Tumour to surrounding muscles ratios regarding hypericin concentration at different times after iv administration of free Hy (▨) or Hy-loaded NPs (■) at a dose of 2 mg/kg to Fischer F-344 rats bearing NuTu-19 tumours. Each data point represents the mean (±SD) of three animals. *Significantly different from ratio of concentration for rats injected with free Hy (Student's t test, $p < 0.05$).

ous micrometastases scattered throughout the abdominal cavity. Fluorescence photodetection (PD) used in combination with surgical resection of malignant tissues might improve recovery. In our study, we evaluated the potential of hypericin-loaded nanoparticles for fluorescence photodetection of ovarian metastases. The purpose was to assess the selective accumulation of entrapped Hy compared to the free drug in ovarian micrometastases.

The choice of animal models used in the PD research is of critical importance for the relevance of pre-clinical studies. The *in vivo* model should be as close as possible to the clinical situation, which in this case is advanced metastatic ovarian cancer. Orthotopic xenografts or chemically induced tumours are presumably the most pertinent models [19,51]. Although NuTu-19 ovarian cancer grafting is not an orthotopic model, the injection in the bursal membrane surrounding the ovaries leads to similar spreading of ovarian tumour nodules [52]. Moreover, tumours have been shown to arise from the appropriate cell type and have the histological characteristics of the most frequent subtype of human ovarian cancer, the poorly differentiated papillary serous ovarian carcinoma [49]. This syngeneic tumour model with a low immunogenicity represents several advantages over orthotopic models developed in nude mice or more frequent subcutaneous xenografts [53]. The latter generally use animals with a lack of immune response that can significantly influence the distribution of the drug [49,51,52] and are suboptimal with respect to the localisation of intraperitoneal metastatic diseases such as ovarian cancer [19,51]. Indeed, the microenvironment of tumours, not reproduced with heterotopic models, is thought to play a crucial role in their development and behaviour [6,54]. For example, molecular signalling pathways using growth-promoting factors such as VEGF, present in high levels in ascites, regulate angiogenesis and permeability of tumour vasculature, cancer cell proliferation, survival, motility and invasion but are also responsible for drug resistance mechanisms. Besides these advantages, the NuTu-19 ovarian cancer model used in this study closely mimics advanced clinical ovarian cancer with the observation of haemorrhagic ascites and the dissemination of metastasis in the peritoneal cavity.

Photodetection using exogenous markers such as Hy has several advantages over endogenous fluorophores [7,19,21], but the main problem restricting the clinical use of mostly lipophilic PS is their systemic administration in an acceptable pharmaceutical solution. Therefore, the design of adequate PS delivery systems is critical for optimising the outcome and acceptability of PD in a clinical context. The formulation of Hy in a biocompatible and stable vehicle is still a challenge and has been widely studied [44,45]. It is obvious that the physical state of a photoactive drug will influence its pharmacokinetics and efficiency. Hy, for example, is known to form aggregates in aqueous solvents. These aggregates will not only affect the fluorescence properties of Hy but also its distribution in the body as shown by Van de Putte et al. [55]. Polymeric nanoparticles help to overcome these delivery and stability problems and enable intravenous administration of Hy. In this study, Hy-loaded PLA NPs were produced with the following properties: (i) mean size of 268 nm, (ii) negative zeta potential, (iii) low residual surfactant and (iv) drug loading of 3.7% (w/w). These NPs were easily administered intravenously to Fischer rats and can thus be used for fluorescence photodetection of ovarian cancer. In the studies using Hy for the photodetection of bladder cancer, the technique of instillation used to administer the drug is described as the main limitation, leading to the exclusion of patients with intravesical clots, diverticula, small bladder capacities or lacking mobility [37,38]. The iv injectable NPs are attractive to avoid the constraint of instillation.

The use of exogenous markers for fluorescence photodetection requires a good selectivity for malignant tissues [56]. The use of nanoparticulate carriers for the passive targeting of tumours by low-molecular weight compounds could be advantageous compared to the free molecule in solution [57]. Indeed, the blood network in tumours is known to be disorganised due to the fast neovascularisation needed to supply oxygen and nutrients to the rapidly growing tissue. Several abnormalities such as defective vascular architecture, higher vascular permeability, large interstitial volume, and lack of lymphatic drainage are well described and exploited for cancer therapy through the so-called enhanced permeability and retention (EPR) effect [58–61]. Our Hy-loaded NPs take advantage of the EPR effect to passively target the ovarian metastases. The leaky vasculature facilitates the extravasation of the 200–300 nm NPs and the impaired lymphatic drainage reduces the NPs clearance from the tumours. As shown by analysis of tumour content (Fig. 3), the NPs were entrapped and retained in ovarian tumours at higher concentrations for an extended period of time (up to 24 h) whereas free Hy was rapidly eliminated from tumours by diffusion. Consequently, entrapping Hy into NPs improved PS availability within tumours and at the same time improved the tumour detection by fluorescence. Moreover, compared to free drug, the NPs did not extravasate from normal vessels and thus lower Hy concentrations were found in the healthy surrounding tissues. This selective accumulation is illustrated by the higher tumour-to-muscle ratios obtained with the NP formulation (Fig. 4). Another drawback with some xenobiotics is their associated toxicity [21,47] and numerous photosensitizers are known to induce skin photosensitivity. The targeted delivery of Hy using PLA NPs resulted in higher bioavailability of the drug at its site of interest, and therefore less side effects are expected. The analysis of tissue content (Figs. 2 and 3) showed a rapid decrease of Hy concentrations in surrounding muscles and other healthy organs when NPs were used. This rapid elimination, in the range of hours, from healthy tissues might help to avoid unwanted photosensitivity reactions and thus a better compliance for patients.

The time interval between drug administration and photodetection is also source of concern [19,21]. Indeed, the optimal time delay after PS administration, corresponding to the high tumour-to-normal tissue ratio, will vary for each PS and for each clinical situation. For this purpose, the NPs could also be beneficial as they offer a larger time window for the fluorescence photodetection. As shown by Hy accumulation in ovarian tumours when NPs were used (Figs. 3 and 4), higher drug amounts were retained in tumours for a longer time than with free Hy. Several methods have been developed to enhance this positive aspect of NPs by increasing the blood circulation time. Indeed, Hy associated with NPs (Fig. 2A) remained longer in the bloodstream than free drug. However, NPs are quickly opsonised, removed from the bloodstream and sequestrated in organs of the reticuloendothelial system (RES) such as the liver and spleen (Fig. 2C) [62]. One major approach to avoid RES tropism, already applied to other PS-loaded NPs, is PEGylation [63–67]. The decoration of our Hy-loaded NPs with PEG moieties could further improve the selective accumulation in ovarian metastases.

Hy is also evaluated as a potential tool for PDT. *In vivo* and *in vivo* studies have demonstrated the photoactivity of Hy [22,23,68,69]. In a previous study, Hy-loaded nanoparticles have been shown to be active after irradiation in NuTu-19 ovarian cancer cells [48]. A major concern with PDT of invasive cancers such as ovarian or bladder cancer is the high risk of normal tissue damage if the PS selectivity for malignant cells is not sufficient. Due to the high dissemination of ovarian tumour nodules, a selective irradiation of each abnormal lesion is impossible, although whole peritoneal cavity irradiation could be considered. To avoid collateral damage, a high selectivity for malignant tissues is crucial and the concept of PDT using Hy-loaded NPs could be promising. Therefore, NPs could also be advantageous for the therapeutic use of Hy.

5. Conclusion

This study provides an *in vivo* proof-of-concept for using Hy-loaded NPs for fluorescence photodetection. Nanoencapsulation of Hy in PLA allows the intravenous administration of this hydrophobic PS. Moreover, higher *in vivo* selective accumulation in malignant ovarian tissues was reached with loaded NPs compared to free drug. Fluorescence detection using Hy-loaded NPs could improve the eradication of the disease by improving the surgical ablation of all detectable tumour nodules. The selectivity of Hy-loaded NPs also favours possible therapeutic approaches using Hy-loaded NPs for PDT.

Acknowledgements

Karl Storz Endoskope is gratefully acknowledged for lending the endoscopy system. The authors thank Brigitte Delavy for her technical help with tissue analysis.

Appendix A. Supplementary data

Supplementary data associated with this article can be found, in the online version, at doi:10.1016/j.ejpb.2008.10.005.

References

[1] R. Sankaranarayanan, J. Ferlay, Worldwide burden of gynaecological cancer: the size of the problem, Best Pract. Res. Clin. Obstet. Gynaecol. 20 (2006) 207–225.
[2] J. Ferlay, P. Autier, M. Boniol, M. Heanue, M. Colombet, P. Boyle, Estimates of the cancer incidence and mortality in Europe in 2006, Ann. Oncol. 18 (2007) 581–592.
[3] A. Jemal, R. Siegel, E. Ward, T. Murray, J. Xu, M.J. Thun, Cancer statistics, 2007, CA Cancer J. Clin. 57 (2007) 43–66.
[4] J.L. Benedet, H. Bender, H.I. Jones, H.Y. Ngan, S. Pecorelli, FIGO staging classifications and clinical practice guidelines in the management of gynecologic cancers. FIGO Committee on Gynecologic Oncology, Int. J. Gynaecol. Obstet. 70 (2000) 209–262.
[5] S.A. Cannistra, Cancer of the ovary, N. Engl. J. Med. 351 (2004) 2519–2529.
[6] H. Naora, D.J. Montell, Ovarian cancer metastasis: integrating insights from disparate model organisms, Nat. Rev. Cancer 5 (2005) 355–366.
[7] M. Stringer, K. Moghissi, Photodiagnosis and fluorescence imaging in clinical practice, Photodiagn. Photodyn. Ther. 1 (2004) 9–12.
[8] S. Denzinger, M. Burger, B. Walter, R. Knuechel, W. Roessler, W.F. Wieland, T. Filbeck, Clinically relevant reduction in risk of recurrence of superficial bladder cancer using 5-aminolevulinic acid-induced fluorescence diagnosis: 8-year results of prospective randomized study, Urology 69 (2007) 675–679.
[9] R. Ackroyd, C. Kelty, N. Brown, M. Reed, The history of photodetection and photodynamic therapy, Photochem. Photobiol. 74 (2001) 656–669.
[10] A.L. Major, G.S. Rose, C.F. Chapman, J.C. Hiserodt, B.J. Tromberg, T.B. Krasieva, Y. Tadir, U. Haller, P.J. DiSaia, M.W. Berns, In vivo fluorescence detection of ovarian cancer in the NuTu-19 epithelial ovarian cancer animal model using 5-aminolevulinic acid (ALA), Gynecol. Oncol. 66 (1997) 122–132.
[11] R. Hornung, A.L. Major, M. McHale, L.H. Liaw, L.A. Sabiniano, B.J. Tromberg, M.W. Berns, Y. Tadir, In vivo detection of metastatic ovarian cancer by means of 5-aminolevulinic acid-induced fluorescence in a rat model, J. Am. Assoc. Gynecol. Laparosc. 5 (1998) 141–148.
[12] M.C. Aalders, H.J. Sterenborg, F.A. Stewart, N. Van der Vange, Photodetection with 5-aminolevulinic acid-induced protoporphyrin IX in the rat abdominal cavity: drug-dose-dependent fluorescence kinetics, Photochem. Photobiol. 72 (2000) 521–525.
[13] J.K. Chan, B.J. Monk, D. Cuccia, H. Pham, S. Kimel, M. Gu, M.J. Hammer-Wilson, L.H. Liaw, K. Osann, P.J. DiSaia, M. Berns, B. Tromberg, Y. Tadir, Laparoscopic photodynamic diagnosis of ovarian cancer using 5-aminolevulinic acid in a rat model, Gynecol. Oncol. 87 (2002) 64–70.
[14] F. Ludicke, T. Gabrecht, N. Lange, G. Wagnieres, H. van den Bergh, L. Berclaz, A.L. Major, Photodynamic diagnosis of ovarian cancer using hexaminolaevulinate: a preclinical study, Br. J. Cancer 88 (2003) 1780–1784.
[15] P. Collinet, F. Sabban, M. Cosson, M.O. Farine, R. Villet, D. Vinatier, S. Mordon, Laparoscopic photodynamic diagnosis of ovarian cancer peritoneal micro metastasis: an experimental study, Photochem. Photobiol. 83 (2007) 647–651.
[16] A.L. Major, F. Ludicke, A. Campana, Feasibility study to detect ovarian cancer micrometastases by fluorescence photodetection, Lasers Med. Sci. 17 (2002) 2–5.
[17] M. Loning, H. Diddens, W. Kupker, K. Diedrich, G. Hüttmann, Laparoscopic fluorescence detection of ovarian carcinoma metastases using 5-aminolevulinic acid-induced protoporphyrin IX, Cancer 100 (2004) 1650–1656.
[18] M.C. Loning, H.C. Diddens, K. Holl-Ulrich, U. Loning, W. Kupker, K. Diedrich, G. Huttmann, Fluorescence staining of human ovarian cancer tissue following application of 5-aminolevulinic acid: fluorescence microscopy studies, Lasers Surg. Med. 38 (2006) 549–554.
[19] G.A. Wagnières, W.M. Star, B.C. Wilson, In vivo fluorescence spectroscopy and imaging for oncological applications, Photochem. Photobiol. 68 (1998) 603–632.
[20] Y.N. Konan, R. Gurny, E. Allemann, State of the art in the delivery of photosensitizers for photodynamic therapy, J. Photochem. Photobiol. B 66 (2002) 89–106.
[21] R.R. Allison, R. Cuenca, G.H. Downie, M.E. Randall, V.S. Bagnato, C.H. Sibata, PD/PDT for gynecological disease: a clinical review, Photodiagn. Photodyn. Ther. 2 (2005) 51–63.
[22] G. Lavie, Y. Mazur, D. Lavie, D. Meruelo, The chemical and biological properties of hypericin – a compound with a broad-spectrum of biological activities, Med. Res. Rev. 15 (1995) 111–119.
[23] P. Agostinis, A. Vantieghem, W. Merlevede, P.A.M. De Witte, Hypericin in cancer treatment: more light on the way, Int. J. Biochem. Cell Biol. 34 (2002) 221–241.
[24] C. Hadjur, M.J. Richard, M.O. Parat, P. Jardon, A. Favier, Photodynamic effects of hypericin on lipid peroxidation and antioxidant status in melanoma cells, Photochem. Photobiol. 64 (1996) 375–381.
[25] C. Hadjur, M.J. Richard, M.O. Parat, A. Favier, P. Jardon, Photodynamically induced cytotoxicity of hypericin dye on human fibroblast cell line MRC5, J. Photochem. Photobiol. B 27 (1995) 139–146.
[26] A.L. Vandenbogaerde, J.F. Cuveele, P. Proot, B.E. Himpens, W.J. Merlevede, P.A. de Witte, Differential cytotoxic effects induced after photosensitization by hypericin, J. Photochem. Photobiol. B 38 (1997) 136–142.
[27] A.L. Vandenbogaerde, A. Kamuhabwa, E. Delaey, B.E. Himpens, W.J. Merlevede, P.A. de Witte, Photocytotoxic effect of pseudohypericin versus hypericin, J. Photochem. Photobiol. B 45 (1998) 87–94.
[28] C.D. Liu, D. Kwan, R.E. Saxton, D.W. McFadden, Hypericin and photodynamic therapy decreases human pancreatic cancer in vitro and in vivo, J. Surg. Res. 93 (2000) 137–143.
[29] B. Chen, P.A. de Witte, Photodynamic therapy efficacy and tissue distribution of hypericin in a mouse P388 lymphoma tumor model, Cancer Lett. 150 (2000) 111–117.
[30] B. Chen, Y. Xu, T. Roskams, E. Delaey, P. Agostinis, J.R. Vandenheede, P. De Witte, Efficacy of antitumoral photodynamic therapy with hypericin: relationship between biodistribution and photodynamic effects in the RIF-1 mouse tumor model, Int. J. Cancer 93 (2001) 275–282.
[31] H.Y. Du, B.H. Bay, M. Olivo, Biodistribution and photodynamic therapy with hypericin in a human NPC murine tumor model, Int. J. Oncol. 22 (2003) 1019–1024.
[32] Z. Diwu, Novel therapeutic and diagnostic applications of hypocrellins and hypericins, Photochem. Photobiol. 61 (1995) 529–539.
[33] M.A. D'Hallewin, L. Bezdetnaya, F. Guillemin, Fluorescence detection of bladder cancer: a review, Eur. Urol. 42 (2002) 417–425.
[34] D. Jocham, H. Stepp, R. Waidelich, Photodynamic diagnosis in urology: state-of-the-art, Eur. Urol. 53 (2007) 1138–1150.
[35] N.E. Stavropoulos, A. Kim, U.U. Nseyo, I. Tsimaris, T.D. Chung, T.A. Miller, M. Redlak, U.O. Nseyo, D. Skalkos, Hypericum perforatum L. extract – novel photosensitizer against human bladder cancer cells, J. Photochem. Photobiol. B 84 (2006) 64–69.
[36] C.L. Saw, M. Olivo, W.W. Chin, K.C. Soo, P.W. Heng, Superiority of *N*-methyl pyrrolidone over albumin with hypericin for fluorescence diagnosis of human bladder cancer cells implanted in the chick chorioallantoic membrane model, J. Photochem. Photobiol. B 86 (2006) 207–218.
[37] M.A. D'Hallewin, P.A. de Witte, E. Waelkens, W. Merlevede, L. Baert, Fluorescence detection of flat bladder carcinoma in situ after intravesical instillation of hypericin, J. Urol. 164 (2000) 349–351.
[38] M.A. D'Hallewin, A.R. Kamuhabwa, T. Roskams, P.A.M. De Witte, L. Baert, Hypericin-based fluorescence diagnosis of bladder carcinoma, BJU Int. 89 (2002) 760–763.
[39] H.G. Sim, W.K. Lau, M. Olivo, P.H. Tan, C.W. Cheng, Is photodynamic diagnosis using hypericin better than white-light cystoscopy for detecting superficial bladder carcinoma?, BJU Int 95 (2005) 1215–1218.
[40] A.P. Castano, T.N. Demidova, M.R. Hamblin, Mechanisms in photodynamic therapy: part three-photosensitizer pharmacokinetics, biodistribution, tumor localization and modes of tumor destruction, Photodiagn. Photodyn. Ther. 2 (2005) 91–106.
[41] A.R. Kamuhabwa, P. Augustijns, P.A. de Witte, In vitro transport and uptake of protohypericin and hypericin in the Caco-2 model, Int. J. Pharm. 188 (1999) 81–86.
[42] A.R. Kamuhabwa, K.R. Geboes, P.A. de Witte, Investigation of the absorption of hypericin into the skin of hairless mice, J. Pharm. Pharmacol. 52 (2000) 487–494.
[43] A.S. Derycke, P.A. de Witte, Liposomes for photodynamic therapy, Adv. Drug Deliv. Rev. 56 (2004) 17–30.
[44] C.L. Saw, M. Olivo, K.C. Soo, P.W. Heng, Delivery of hypericin for photodynamic applications, Cancer Lett. 241 (2005) 23–30.
[45] A. Huygens, A.R. Kamuhabwa, P.A. de Witte, Stability of different formulations and ion pairs of hypericin, Eur. J. Pharm. Biopharm. 59 (2005) 461–468.
[46] C.L. Saw, M. Olivo, K.C. Soo, P.W. Heng, Spectroscopic characterization and photobleaching kinetics of hypericin-*N*-methyl pyrrolidone formulations, Photochem. Photobiol. Sci. 5 (2006) 1018–1023.
[47] M. Zeisser-Labouèbe, A. Vargas, F. Delie, Nanoparticles for photodynamic therapy of cancer, in: C.S. Kumar (Ed.), Nanomaterials for Cancer Therapy, Wiley-VCH, Weinheim, 2006, pp. 40–86.

[48] M. Zeisser-Labouèbe, N. Lange, R. Gurny, F. Delie, Hypericin-loaded nanoparticles for the photodynamic treatment of ovarian cancer, Int. J. Pharm. 326 (2006) 174–181.
[49] G.S. Rose, L.M. Tocco, G.A. Granger, P.J. DiSaia, T.C. Hamilton, A.D. Santin, J.C. Hiserodt, Development and characterization of a clinically useful animal model of epithelial ovarian cancer in the Fischer 344 rat, Am. J. Obstet. Gynecol. 175 (1996) 593–599.
[50] Y.N. Konan, R. Cerny, J. Favet, M. Berton, R. Gurny, E. Allemann, Preparation and characterization of sterile sub-200 nm meso-tetra(4-hydroxylphenyl)porphyrin-loaded nanoparticles for photodynamic therapy, Eur. J. Pharm. Biopharm. 55 (2003) 115–124.
[51] M.A. D'Hallewin, S. Berrahmoune, L. Bezdetnaya, H.P. Lassalle, F. Guillemin, Orthotopic animal models for oncologic photodynamic therapy and photodiagnosis, Photodiagn. Photodyn. Ther. 4 (2007) 230–236.
[52] S. Sale, S. Orsulic, Models of ovarian cancer metastasis: murine models, Drug Discov. Today: Disease Models 3 (2006) 149–154.
[53] B.A. Teicher, Tumor models for efficacy determination, Mol. Cancer Ther. 5 (2006) 2435–2443.
[54] W.L. Monsky, C.M. Carreira, Y. Tsuzuki, T. Gohongi, D. Fukumura, R.K. Jain, Role of host microenvironment in angiogenesis and microvascular functions in human breast cancer xenografts: mammary fat pad versus cranial tumors, Clin. Cancer Res. 8 (2002) 1008–1013.
[55] M. Van de Putte, T. Roskams, G. Bormans, A. Verbruggen, P.A. de Witte, The impact of aggregation on the biodistribution of hypericin, Int. J. Oncol. 28 (2006) 655–660.
[56] N. Lange, Controlled drug delivery in photodynamic therapy and fluorescence-based diagnosis of cancer, in: M.-A. Mycek, B.W. Pogue (Eds.), Handbook of Biomedical Fluorescence, Marcel Decker, Inc., New York N.Y., 2003, pp. 563–635.
[57] I. Brigger, C. Dubernet, P. Couvreur, Nanoparticles in cancer therapy and diagnosis, Adv. Drug Deliv. Rev. 54 (2002) 631–651.
[58] Y. Takakura, R.I. Mahato, M. Hashida, Extravasation of macromolecules, Adv. Drug Deliv. Rev. 34 (1998) 93–108.
[59] H. Maeda, J. Wu, T. Sawa, Y. Matsumura, K. Hori, Tumor vascular permeability and the EPR effect in macromolecular therapeutics: a review, J. Control Release 65 (2000) 271–284.
[60] H. Maeda, J. Fang, T. Inutsuka, Y. Kitamoto, Vascular permeability enhancement in solid tumor: various factors, mechanisms involved and its implications, Int. Immunopharmacol. 3 (2003) 319–328.
[61] A.K. Iyer, G. Khaled, J. Fang, H. Maeda, Exploiting the enhanced permeability and retention effect for tumor targeting, Drug Discov. Today 11 (2006) 812–818.
[62] D.E.I. Owens, N.A. Peppas, Opsonization, biodistribution, and pharmacokinetics of polymeric nanoparticles, Int. J. Pharm. 307 (2006) 93–102.
[63] E. Allemann, N. Brasseur, O. Benrezzak, J. Rousseau, S.V. Kudrevich, R.W. Boyle, J.C. Leroux, R. Gurny, J.E. van Lier, PEG-coated poly(lactic acid) nanoparticles for the delivery of hexadecafluoro zinc phthalocyanine to EMT-6 mouse mammary tumours, J. Pharm. Pharmacol. 47 (1995) 382–387.
[64] E. Allemann, J. Rousseau, N. Brasseur, S.V. Kudrevich, K. Lewis, J.E. van Lier, Photodynamic therapy of tumours with hexadecafluoro zinc phthalocynine formulated in PEG-coated poly(lactic acid) nanoparticles, Int. J. Cancer 66 (1996) 821–824.
[65] R. Hornung, M.K. Fehr, J. Monti-Frayne, T.B. Krasieva, B.J. Tromberg, M.W. Berns, Y. Tadir, Highly selective targeting of ovarian cancer with the photosensitizer PEG-m-THPC in a rat model, Photochem. Photobiol. 70 (1999) 624–629.
[66] O. Bourdon, V. Mosqueira, P. Legrand, J. Blais, A comparative study of the cellular uptake localization and phototoxicity of meta-tetra(hydroxyphenyl) chlorin encapsulated in surface-modified submicronic oil/water carriers in HT29 tumor cells, J. Photochem. Photobiol. B 55 (2000) 164–171.
[67] O. Bourdon, I. Laville, D. Carrez, A. Croisy, P. Fedel, A. Kasselouri, P. Prognon, P. Legrand, J. Blais, Biodistribution of meta-tetra(hydroxyphenyl)chlorin incorporated into surface-modified nanocapsules in tumor-bearing mice, Photochem. Photobiol. Sci. 1 (2002) 709–714.
[68] H. Koren, G.M. Schenk, R.H. Jindra, G. Alth, R. Ebermann, A. Kubin, G. Koderhold, M. Kreitner, Hypericin in phototherapy, J. Photochem. Photobiol. B 36 (1996) 113–119.
[69] A. Kamuhabwa, P. Agostinis, B. Ahmed, W. Landuyt, B. Van Cleynenbreugel, H. Van Poppel, P. De Witte, Hypericin as a potential phototherapeutic agent in superficial transitional cell carcinoma of the bladder, Photochem. Photobiol. Sci. 3 (2004) 772–780.